Electronic Supplementary Information (ESI) for Chemical Communications.

Supporting Information

In situ fluorescence imaging reveals mitochondrial H$_2$O$_2$ mediates lysosomal dysfunction in depression

Xin Wang,[‡a] Qi Ding,[‡a] Ying Tian,[a] Wei Wu,[*b] Feida Che,[a] Ping Li,[*a] Wen Zhang,[a] Wei Zhang[a] and Bo Tang[*a]

[a]College of Chemistry, Chemical Engineering and Materials Science, Collaborative Innovation Center of Functionalized Probes for Chemical Imaging in Universities of Shandong, Key Laboratory of Molecular and Nano Probes, Ministry of Education, Institutes of Biomedical Sciences, Shandong Normal University, Jinan 250014, People's Republic of China.

[b]Department of Neurology, Qi-Lu Hospital of Shandong University and Brain Science Research Institute, Shandong University Jinan, Shandong 250012, P.R. China.

*E-mail: tangb@sdnu.edu.cn., lip@sdnu.edu.cn., drwuwei@126.com.

Experimental Procedures

Materials and reagents

All reagents were purchased commercially and used without further purification. 2,4-dihydroxybenzaldehyde, 1,6-Dihydroxy Naphthalene, Methanesulfonic acid, Cesium Carbonate, Corticosterone were from Shanghai Macklin Biochemical Co., Ltd. 2-morpholin-4-ylethanamine, 4-(Bromomethyl) benzeneboronicacidpinacolester were from Shanghai Aladdin Bio-Chem Technology Co., Ltd. 3-(4,5-Dimethylthiazol-2-yl)-2,5-diphenyltetrazolium bromide (MTT) was from Sigma-Aldrich. Silicagel plates (HSGF-254 20*20 cm) for TLC were from Yantai Jiangyou silicon development Co., Ltd. PC12 were purchased from Cell Bank of the Chinese Academy of Sciences (Shanghai, China). The C57BL/6J mice (age: 6 weeks; average body weight: 20 ± 2 g) were purchased from Shandong University Laboratory Animal Center. All the animal experiments were carried out in accordance with the relevant laws and guidelines issued by the Ethical Committee of Shandong University.

Instruments

^{1}H NMR spectra were obtained at 400 MHz using Bruker NMR spectrometers, and ^{13}C NMR spectra were recorded at 100 MHz. The mass spectra were obtained using the Bruker maXis ultra-high-resolution-TOF MS system. Absorption spectra were measured on an Evolution 220 UV-vis spectrophotometer (Thermo Scientific Co., Ltd.). All fluorescence measurements were carried out at room temperature on an F-4600 fluorescence spectrometer. Absorbance was measured in a microplate reader (RT 6000, Rayto, USA) in the MTT assay. Fluorescence imaging in cells were performed with Leica TCS SP8 Confocal Laser Scanning Microscope. Animals imaging was performed by the Zeiss LSM 880 NLO with a 20× water objective. Force swimming test and tail Suspension test were analyzed with DepressionScan (Clever Sys. Inc.).

Cell culture

PC12 cells were cultured in RPMI 1640 supplemented with 10 % fetal bovine serum, 1 % penicillin and 1 % streptomycin at 37 °C (w/v) in an MCO-15AC incubator (SANYO, Tokyo, Japan) in 5 % CO_2 95 % air. One day before imaging, the cells were detached and placed in glass-bottomed dishes.

Determination of the detection limit

The detection limit was determined from the fluorescence titration data. The detection limit was calculated with the following equation: Detection limit = $3\sigma/k$, where σ is the standard deviation of blank measurement, k is the slope between the fluorescence intensity versus H_2O_2 concentration.

Reactive oxygen species preparation and determination

Reactive oxygen species (ROS) were prepared according to methods adapted from previous reports[1, 2]. $O_2^{\bullet-}$ was produced from KO_2 in DMSO solution by an ultrasonic method. Hydrogen peroxide (H_2O_2), tert-butylhydroperoxide (TBHP), and hypochlorite (NaClO) were acquired from 30 %, 70 %, and 10 % aqueous solutions, respectively. The hydroxyl radical (•OH) was generated by the reaction of 1.0 mM $FeCl_2$ with a 200 μM H_2O_2 aqueous solution. Nitric oxide (NO) was obtained from a stock solution prepared with sodium nitroprusside. Singlet oxygen ($^1O_2$) was prepared with the NaClO-H_2O_2 system. The concentrations of the ROS/reactive nitrogen species (RNS)[3-7] were determined as follows:

1. $O_2^{\bullet-}$: λ_{abs}=250 nm, ε=2682 L mol^{-1} cm^{-1}
2. H_2O_2: λ_{abs}=240 nm, ε=43.6 L mol^{-1} cm^{-1}

3. TBHP: Iodometry

4. ClO⁻: λ_{abs}=209 nm, ε=350 L mol^{-1} cm^{-1}

5. •OH: Measurement of the production of methane sulfinic acid in a reaction with DMSO (420 nm) by colorimetric assay

6. NO: Griess method

7. $^1O_2$: Measurement of the reaction with 1,3-diphenylisobenzofuran (410 nm) by colorimetric assay

Notes: λ_{abs} is the absorption spectrum, and ε is the molar extinction coefficient.

Cells imaging

For cells imaging, living PC12 cells were detached, transplanted onto glass-bottomed dishes, and cultured for 24 h before imaging. After an incubation with the probe for 40 min, the cell culture media were removed and cells were washed with 1.0 mL PBS for three times. Fluorescence images of LY-H$_2$O$_2$ were obtained with an excitation wavelength of 405 nm and blue channel was 410 nm-500 nm by using the Leica TCS SP8 Confocal Laser Scanning Microscope. Fluorescence images of MI-H$_2$O$_2$ were obtained with an excitation wavelength of 633 nm and right channel was 650 nm-750 nm by using the Leica TCS SP8 Confocal Laser Scanning Microscope. Analyses were performed using Leica software. For data analysis, the average fluorescence intensity per image under each experimental condition was obtained by selecting regions of interest. Each experiment was repeated at least three separate times with identical results.

In vivo **imaging**

In the brain imaging experiment, Zeiss 880 NLO microscopy was employed with z-stack mode and a water objective (20X). At first, the mice were anesthetized by chloral hydrate, then the mice labeled with 0.3 mg kg^{-1} LY-H$_2$O$_2$ and 0.6 mg kg^{-1} MI-H$_2$O$_2$ *via* intraperitoneal injection. After 30 minutes, the mice brain images were acquired using the Zeiss 880 NLO microscopy with a blue channel (λ_{ex} = 800 nm and λ_{em} = 414 nm-501 nm) and a red channel (λ_{ex} = 633 nm and λ_{em} = 643 nm-722 nm). Analyses were performed using Zeiss software. For data analysis, the average fluorescence intensity per image under each experimental condition was obtained by selecting regions of interest. Each experiment was repeated at least three separate times with identical results.

Cytotoxicity assays

The cytotoxicity was measured by 3-(4,5-dimethylthiazol-2-yl)-2,5-diphenyltetrazolium bromide (MTT) assay. PC12 cells were seeded in a 96-well plate at a concentration of 1×10^5 cells well^{-1} in 100 μL of Roswell Park Memorial Institute (RPMI-1640) medium with 10 % fetal bovine serum, 1 % penicillin, and 1 % streptomycin and maintained at 37 °C in a 5 % CO$_2$ incubator for 12 h. Then, cells were exposed to different concentrations of LY-H$_2$O$_2$ and MI-H$_2$O$_2$ (1×10^{-6}, 5×10^{-6}, 1×10^{-5}, 2×10^{-5}, 5×10^{-5}, 2×10^{-4}, 5×10^{-4} M) for 24 h. The total volume of 96-well microtiter plates is 200 μL well^{-1}. The cells were washed with 37 °C PBS and MTT solution (5 mg mL^{-1}, 20 μL) was added to each well and continuously incubated for 4 h at 37 °C. After 4 h, MTT solution was removed and DMSO (150 μL) was added to each well to dissolve the dark blue formazan crystals. Absorbance was measured at 490 nm in a Triturus microplate reader.

Proteomic analysis

Glucocerebrosidase was incubated for 2 h at 37 °C in Buffer A (50 mM sodium phosphate, pH = 7.4) supplemented with 2 mM H$_2$O$_2$. Then glucocerebrosidase was subjected to Tyrisin digestion, the peptides were isolated from the hydrolysate by solid phase extraction on a C-18 column. Then

proteomic analysis was performed through LC-MS/MS.

Mouse models with depression-like behaviors

Six-week-old C57 male mice were used to construct depression models, and the mice were divided into normal groups and depression groups. Mice in the depression group were provided with water containing corticosterone (CORT) for 3 weeks, and mice in the normal group were provided with ordinary water for 3 weeks.

Preparation of corticosterone solution: 5 mg of corticosterone was dissolved in 5 ml of absolute ethanol, and then diluted with water to 500 ml.

Sucrose preference test

Sucrose preference test was conducted using a two-bottle choice procedure before and after chronic-restraint stress procedure.[8] Before the sucrose preference test (SPT), mice were habituated to drink a 1 % sucrose solution for 24 h with two bottles. Then, the sucrose solution was replaced with water for an additional 24 h. At the start of the test, mice were given access to the two bottles, one filled with sucrose solution and the other with water. The position of the water and sucrose bottles (left or right) was switched every 12 h for two days. Then the mice were left undisturbed, and their overnight fluid consumption was measured at the next morning. The volume of sucrose or water of every bottle was recorded. The sucrose preference was defined as the ratio of the volume of sucrose to the total volume of sucrose and water consumed.

Forced swimming test

Forced swimming test (FST) as a 2 days program were carried out following references.[9] In the FST, each mouse was placed in a cylindrical tank (24 cm height × 10 cm diameter) filled to 6 cm with water at a temperature of 24 ± 1 °C. The mice could swim freely. On the first day, the mice represented an escape-like behaviors and found an immobility posture that they could maintain their head above water easily for conserving energy. After rested for 24 h, mice would stay immobile quickly. The mice were subjected to 6 min of swimming, but only the last four minutes were considered in the analysis.

Tail suspension test

In the tail suspension test (TST), each mouse was suspended by the tail using adhesive scotch tape from a hook connected to a strain gauge that detected all the movements of the mouse and transmitted them to a central unit, which calculated the total duration of immobility during a 6-min test. However, only the last four minutes were considered in the analysis.

Statistical analysis

All data are expressed as the mean ± S.D. The data under each condition were accumulated from at least three independent experiments. For each experiment, unless otherwise noted, n represents the number of individual biological replicates. For each biological replicate and for all in vitro and ex vivo studies, n ≥ 3. The statistical analyses were performed using Student's t-test. $P < 0.05$ was considered statistically significant.

Data availability

All relevant data that support the findings of this study are available from the corresponding author upon reasonable request.
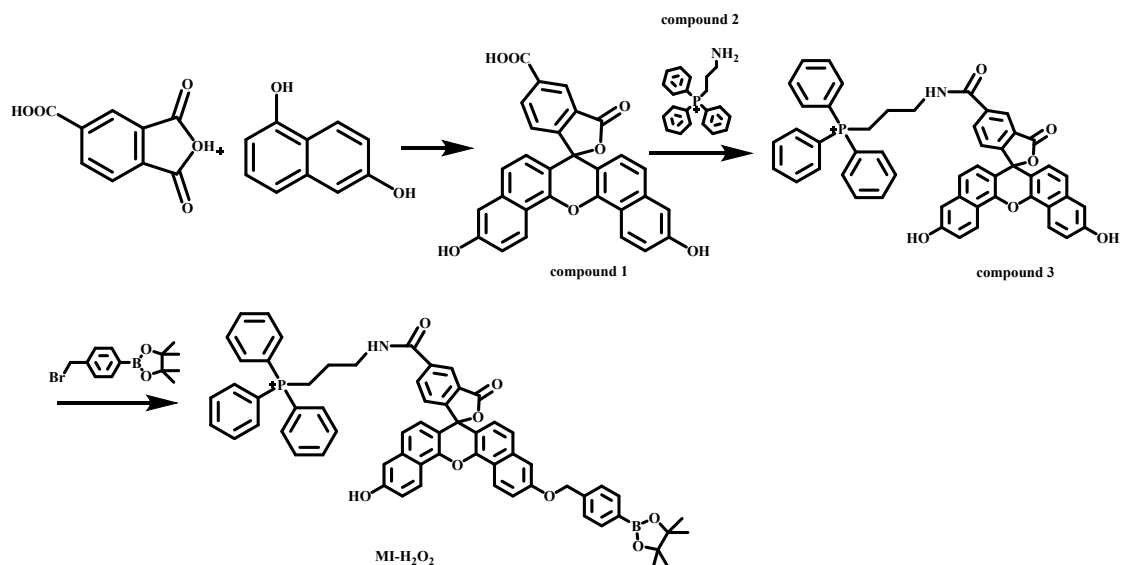
Supplemental Figures

Figure S1 Synthesis scheme of MI-H$_2$O$_2$

Synthesis of the MI-H$_2$O$_2$.

Compounds 1, 2 were synthesized as previously reported in Reference 10.

Compound 3: Compound 1 (0.1 g, 0.2 mmol) and compound 2 (0.1 g, 0.2 mmol) were added to 10 mL of CH$_2$Cl$_2$ and 10 drops of DMF, and then add 4-dimethylaminopyridine (0.03 g, 0.25 mmol) and N, N-Dicyclohexylcarbodiimide (0.05 g, 0.25 mmol), overnight at room temperature under nitrogen protection to obtain compound 3. HRMS (ESI), m/z calcd for C$_{50}$H$_{37}$NO$_6$P$^+$ [M+H]$^+$ 779.2431, found 779.2413.

Compound MI-H$_2$O$_2$: compound 4 (0.38 g, 0.5 mmol) and 4-bromomethylphenylboronic acid pinacolate (0.297 g, 1 mmol) were added to 10 mL of acetonitrile, then add cesium carbonate (0.652 g, 2 mmol), and reflux at 80°C for 18 hours, the crude product was purified by TLC using n-propanol/ammonia (volume ratio 10:1) as the eluent to obtain MI-H$_2$O$_2$. (0.135 g, yield 33.3 %). ^{1}H NMR (400 MHz) δ 8.19 (d, J = 7.8 Hz, 3H), 7.55 (d, J = 7.6 Hz, 3H), 7.15 (d, J = 7.8 Hz, 3H), 6.95 (d, J = 7.8 Hz, 3H), 5.26 (s, 3H), 4.90 (s, 16H), 3.34 (s, 2H), 3.33-3.27 (m, 7H), 3.22 (s, 8H), 1.89 (s, 1H), 1.28 (s, 3H). ^{13}C NMR (100 MHz) δ 160.05, 156.55, 141.61, 133.77, 130.55, 129.45, 127.64, 125.98, 107.54, 61.17, 59.08, 38.91, 35.15, 31.67, 29.43, 28.92, 26.71, 25.53, 22.85, 22.33, 13.06. HRMS (ESI), m/z calcd for C$_{63}$H$_{54}$BNO$_8$P$^+$ [M+H]$^+$ 995.3675, found 995.3628.
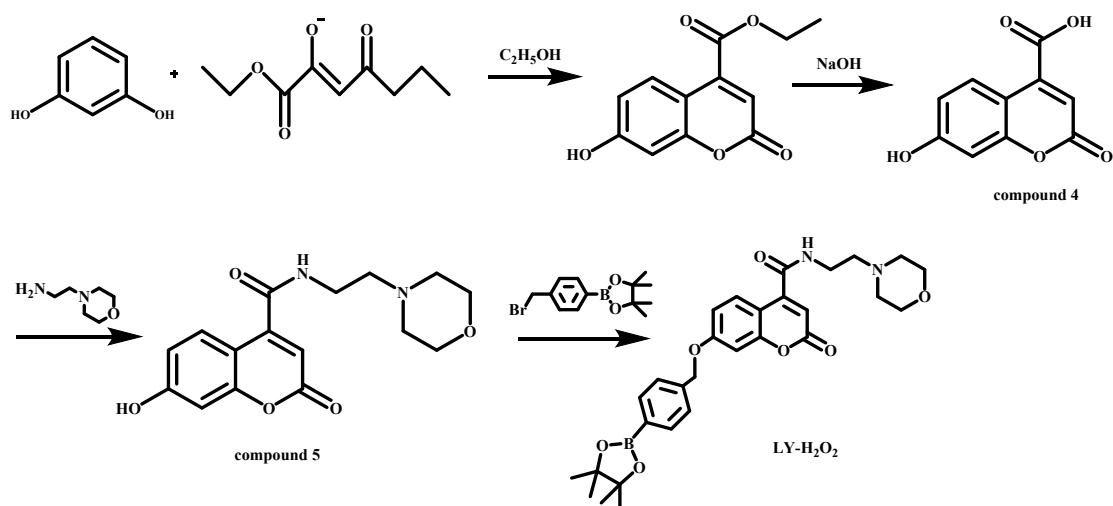
Figure S2 Synthesis scheme of LY-H$_2$O$_2$

Synthesis of the LY-H$_2$O$_2$.

Compounds 4 were synthesized as previously reported in Reference 11.

Compound 5: Compound 4 and N-(2-aminoethyl)morpholine (120 μL, 0.5 mmol) were added to 10 mL of CH$_2$Cl$_2$ and 10 drops of DMF, and then add 4-dimethylamino Pyridine (0.09 g, 0.75 mmol) and N, N-dicyclohexylcarbodiimide (0.15 g, 0.75 mmol), overnight at room temperature under nitrogen protection, the crude product is dichloromethane/methanol (volume ratio 10:1) As an eluent, purified by TLC to obtain compound 5. HRMS (ESI), m/z calcd for C$_{16}$H$_{18}$N$_2$O$_5$ [M-H]$^-$ 317.1132, found 317.1137.

Compound LY-H$_2$O$_2$: compound 5 (0.02 g, 0.06 mmol) and 4-bromomethylphenylboronic acid pinacolate (0.0356 g, 0.12 mmol) were added to 10 mL of acetonitrile, then add cesium carbonate (0.078 g, 0.24 mmol), and reflux at 80 °C for 18 hours, the crude product was purified by TLC using n-propanol/ammonia (volume ratio 10:1) as the eluent to obtain LY-H$_2$O$_2$. ^{1}H NMR (400 MHz,) δ 8.23 (t, J = 7.6 Hz, 2H), 7.72 (d, J = 8.0 Hz, 1H), 7.57 (d, J = 7.8 Hz, 1H), 7.30 (d, J = 7.6 Hz, 1H), 7.19 (d, J = 7.8 Hz, 1H), 7.05-6.88 (m, 2H), 5.32 (d, J = 32.8 Hz, 2H), 4.89 (s, 3H), 3.34 (s, 1H), 3.33-3.13 (m, 6H), 1.26 (s, 8H), 1.20 (s, 6H). ^{13}C NMR (100 MHz) δ 156.58, 156.53, 141.80, 141.67, 134.61, 133.79, 126.84, 126.13, 107.75, 107.61, 61.13, 60.57, 47.46, 47.25, 47.03, 39.07, 39.02, 24.26, 23.77. HRMS (ESI), m/z calcd for C$_{29}$H$_{35}$BN$_2$O$_7$ [M-H]$^-$ 533.2458, found 533.2463.
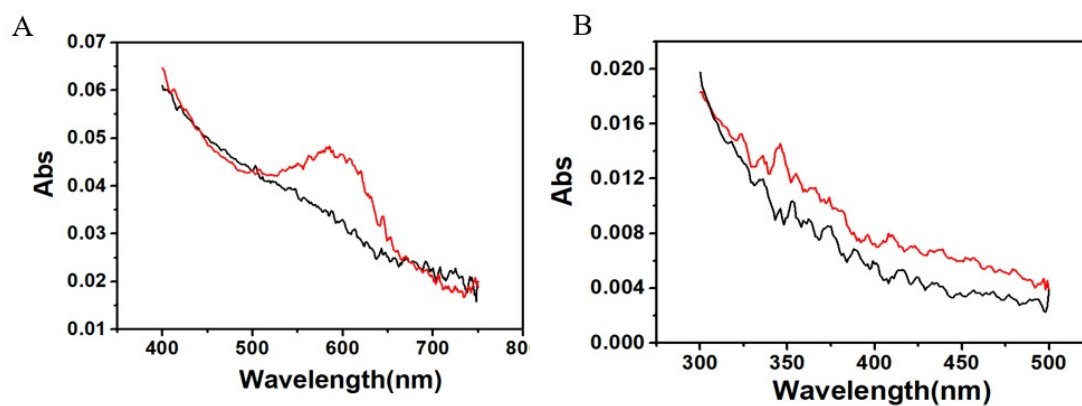
Figure S3 UV-vis absorptions of MI-H$_2$O$_2$ and LY-H$_2$O$_2$ (A) The absorption spectra for MI-H$_2$O$_2$ (120 µM) before (black) and after (red) the addition of H$_2$O$_2$ (100 µM) at pH 8.8 in Hepes buffer. (A) The absorption spectra for LY-H$_2$O$_2$ (120 µM) before (black) and after (red) the addition of H$_2$O$_2$ (100 µM) at pH 4.5 in acetic acid-sodium acetate buffer.
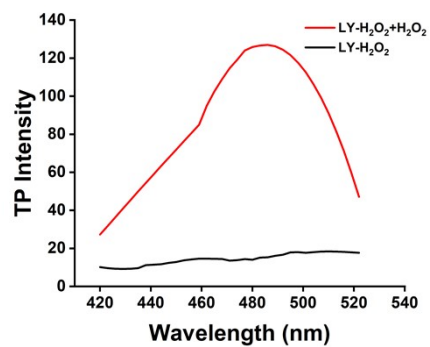
Figure S4 Two-photon fluorescence spectra of LY-H_2O_2. Black line: 120 µM LY-H_2O_2. Red line: 120 µM LY-H_2O_2 reacted with 100 µM H_2O_2. The spectrum was acquired in acetic acid-sodium acetate buffer (pH 4.5) at λ_{ex} = 800 nm.
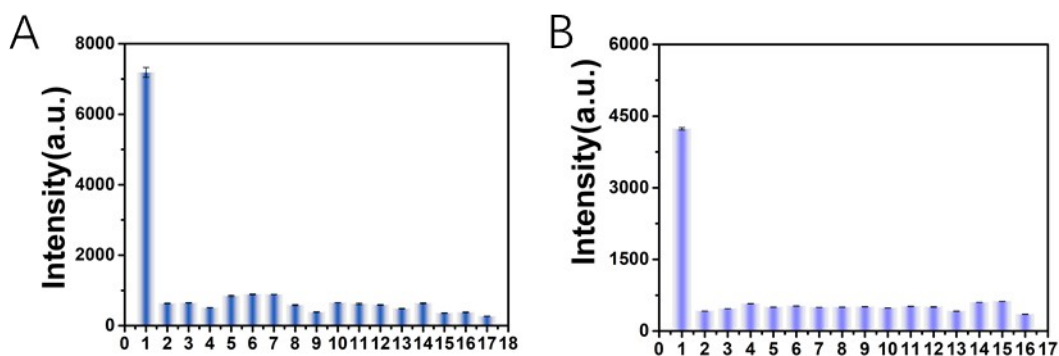
Figure S5 (A) Fluorescence responses of 120 μM MI-H_2O_2 with various ROS, RNS and metals (1. 100 μM H_2O_2, 2. Blank, 3. 200 mM NO, 4. 200 mM •OH, 5. 100 μM TBHP, 6. 20 μM $O_2^{•-}$, 7. 200 μM $^1O_2$, 8. 200 μM NaClO, 9. 10 mM Ca^{2+}, 10. 100 μM Cu^{2+}, 11. 100 μM Cu^+, 12. 10 mM K^+, 13. 10 mM Mg^{2+}, 14. 10 mM Na^+, 15. 100 μM Fe^{2+}, 16. 100 μM Fe^{3+}, 17. 1 mM Zn^{2+}). (B) Fluorescence responses of 120 μM LY-H_2O_2 with various ROS, RNS and metals （1. 100 μM H_2O_2, 2. Blank, 3. 10 mM K^+, 4. 10 mM Mg^{2+}, 5. 10 mM Na^+, 6. 1 mM Zn^{2+}, 7. 100 μM Fe^{2+}, 8. 100 μM Fe^{3+}, 9. 100 μM Cu^+, 10. 100 μM Cu^{2+}, 11. 10 mM Ca^{2+}, 12. 200 mM NO, 13. 100 μM TBHP, 14. 200 μM NaClO, 15. 200 mM •OH, 16. 20 μM $O_2^{•-}$.
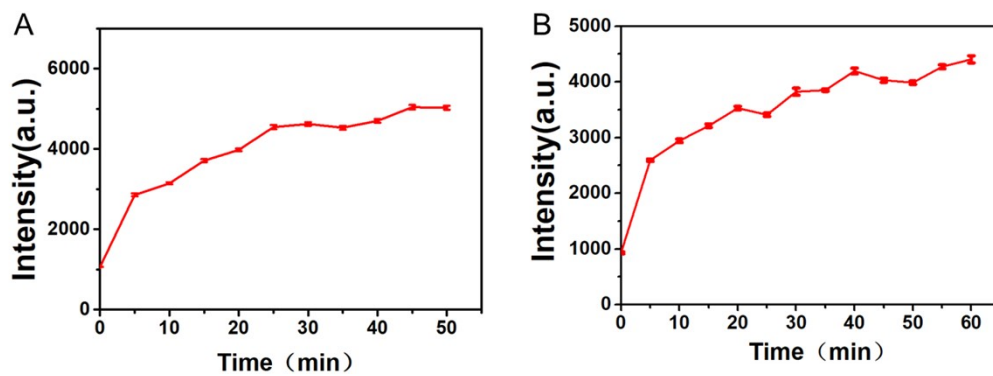
Figure S6 Kinetics experiments of MI-H_2O_2 and LY-H_2O_2. (A) Kinetics curve of MI-H_2O_2 after reaction with 100 μM H_2O_2 at pH 8.8 in HEPES buffer. $\lambda_{ex}/\lambda_{em}$ = 600/670 nm. (B) Kinetics curve of LY-H_2O_2 after reaction with 100 μM H_2O_2 at pH 4.5 in acetic acid-sodium acetate buffer solution. $\lambda_{ex}/\lambda_{em}$ = 360/445 nm.
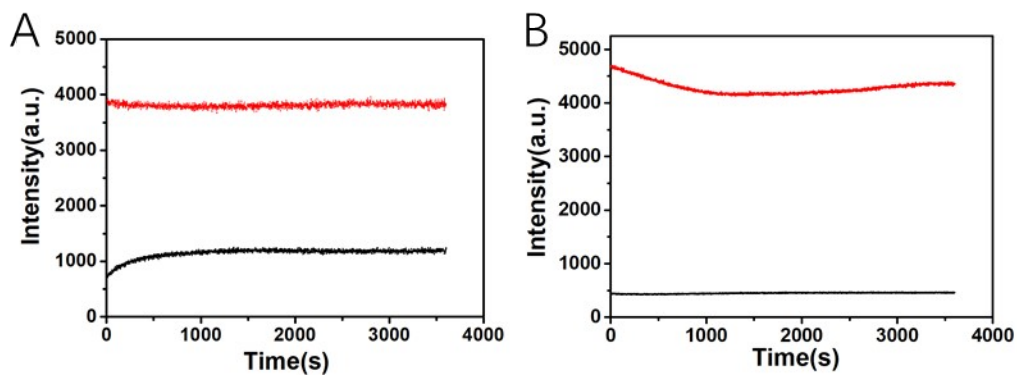
Figure S7 (A) The photostability experiments of 120 μM MI-H$_2$O$_2$ before (black) and after (red) the addition of H$_2$O$_2$ (100 μM) at pH 8.8 in HEPES buffer. (B) The photostability experiments of 120 μM LY-H$_2$O$_2$ before (black) and after (red) the addition of 100 μM H$_2$O$_2$ at pH 4.5 in acetic acid-sodium acetate buffer.
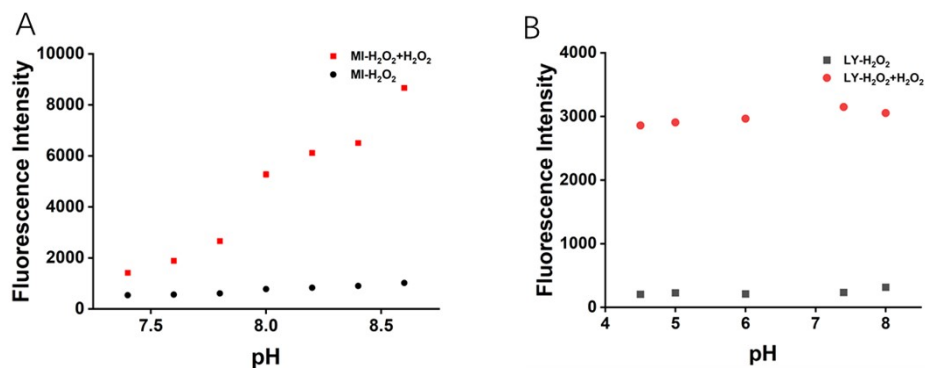
Figure S8 (A) Fluorescence spectra of 120 μM MI-H$_2$O$_2$ (black blots) alone and after the addition of 100 μM H$_2$O$_2$ (red squares) in the presence of a solution with various pH values at λ_{ex} = 600 nm and λ_{em} = 670 nm. (B) Fluorescence spectra of 120 μM LY-H$_2$O$_2$ (black squares) alone and after the addition of 100 μM H$_2$O$_2$ (red blots) in the presence of a solution with various pH values at λ_{ex} = 360 nm and λ_{em} = 445 nm.

A

B
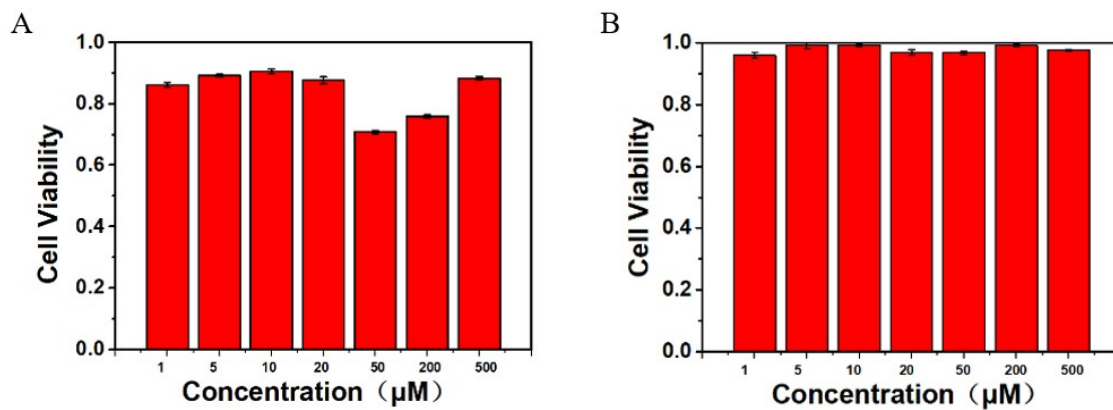
Figure S9 (A) The MTT assay of MI-H_2O_2. The IC_{50} of MI-H_2O_2 is 1981 μM. (B) The MTT assay of LY-H_2O_2. The IC_{50} of LY-H_2O_2 is 868.96 μM.
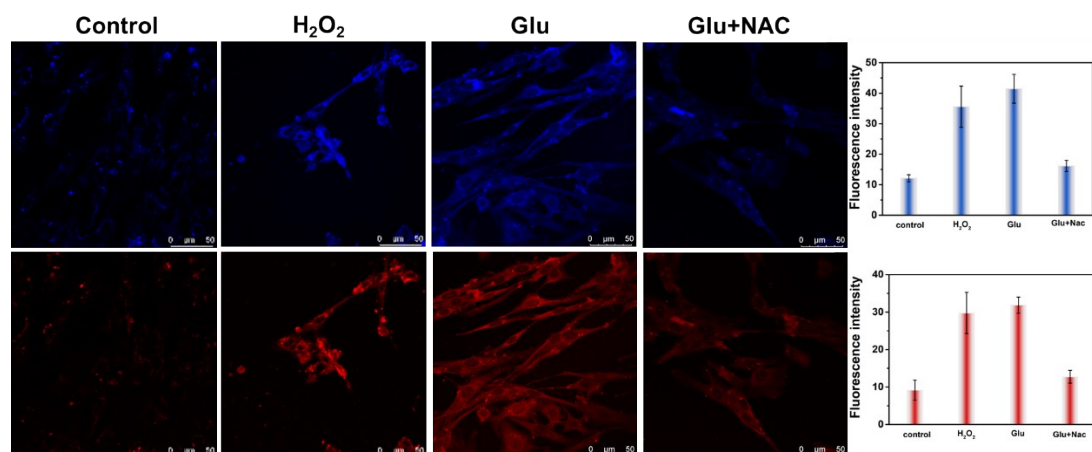
Figure S10 Fluorescence imaging of H_2O_2 in PC12 cells. Control: PC12 cells were incubated with 100 μM MI-H_2O_2 and LY-H_2O_2 for 40 min. H_2O_2: PC12 cells were pretreated with 200 μM H_2O_2 for 60 min and then incubated with 100 μM MI-H_2O_2 and LY-H_2O_2 for 40 min. Glu: PC12 cells were incubated with 100 μM MI-H_2O_2 and LY-H_2O_2 for 40 min after preincubation with 10 mM glutamate for 12 h. Glu+NAC: PC12 cells were pretreated with 10 mM glutamate for 12 h and loaded with 1 mM NAC for 60 min, then cells were incubated with 100 μM MI-H_2O_2 and LY-H_2O_2 for 40 min. The blue channel represented lysosome (λ_{ex}= 405 nm, λ_{em}= 410-500 nm). The red channel represented mitochondria (λ_{ex} = 633 nm, λ_{em} = 650 nm-750 nm). Scale bar = 50 μm. The data are expressed as mean ± S.D.

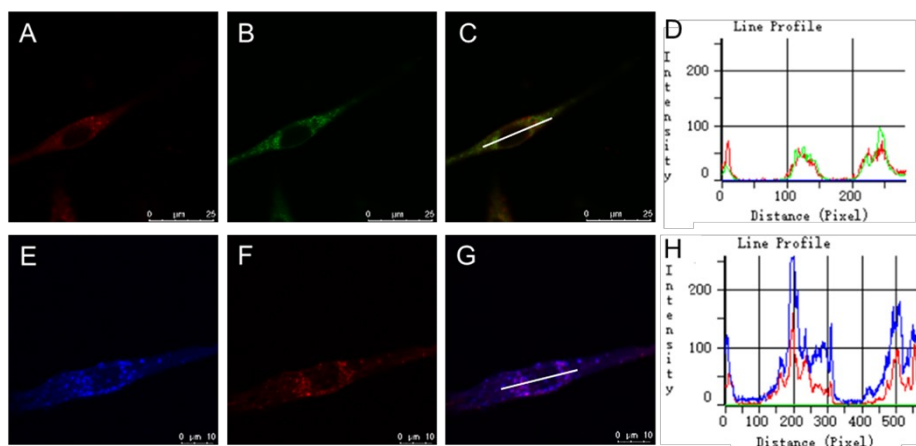**Fig. S11** Co-localization fluorescence images of PC12 cells. (A) Fluorescence image of MI-H_2O_2 (100 μM, λ_{ex} = 633 nm, λ_{em} = 650 nm-750 nm). (B) Fluorescence image of Mito-Tracker Green (100 nM, λ_{ex} = 488 nm, λ_{em} = 495 nm-550 nm). (C) Overlay image of panels A and B. Scale bar = 25 μm. (D) Intensity profile of the white line in image C. (E) Fluorescence image of LY-H_2O_2 (100 μM, λ_{ex} = 405 nm, λ_{em} = 410 nm-500 nm). (F) Fluorescence image of Lyso-Tracker Deep Red (100 nM, λ_{ex} = 633 nm, λ_{em} = 650 nm-750 nm). (G) Overlay image of panels E and F. Scale bar = 10 μm. (H) Intensity profile of the white line in image G.
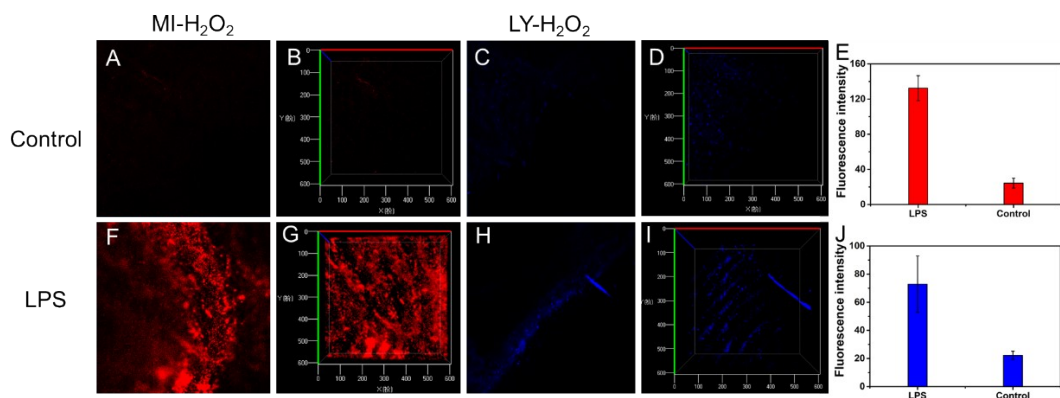
Figure S12 *In vivo* TP imaging at the different depths and the 3D distribution of H_2O_2 in the LPS model and normal mice pretreated with MI-H_2O_2 (0.6 mg kg^{-1}) and LY-H_2O_2 (0.3 mg kg^{-1}) for 15 min. (A) MI-H_2O_2 imaging at 120 μm in the abdominal cavity of normal mice. (B) The 3D images of MI-H_2O_2 images of different depths in the abdominal cavity of mice with normal mice are superimposed in the Z direction. (C) MI-H_2O_2 imaging at 40 μm in the abdominal cavity of normal mice. (D) The 3D images of MI-H_2O_2 images of different depths in the abdominal cavity of mice with normal mice are superimposed in the Z direction. (E) The fluorescence intensities of panels A and F. (F) MI-H_2O_2 imaging at 120 μm in the abdominal cavity of mice with LPS-induced inflammation. (G) The 3D images of MI-H_2O_2 images of different depths in the abdominal cavity of mice with LPS-induced inflammation are superimposed in the Z direction. (H) LY-H_2O_2 imaging at 180 μm in the abdominal cavity of mice with LPS-induced inflammation. (I) The 3D images of LY-H_2O_2 images of different depths in the abdominal cavity of mice with LPS-induced inflammation are superimposed in the Z direction. (J) The fluorescence intensities of parts C and H. Red channel: λ_{ex} = 633 nm, λ_{em} = 643 nm-722 nm. Blue channel: λ_{ex} = 800 nm，λ_{em} = 414 nm-501 nm.
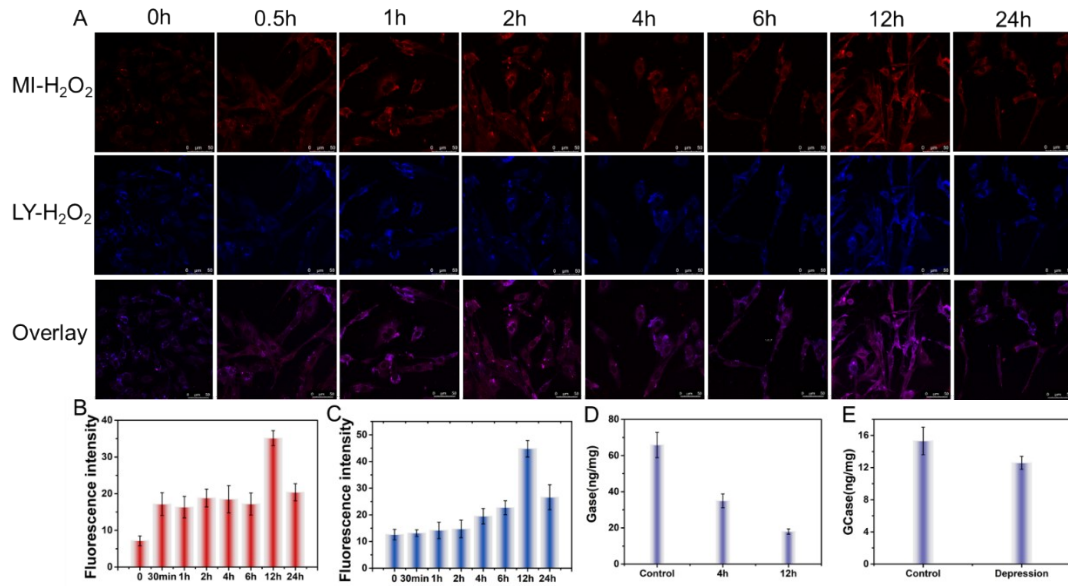
Figure S13 Confocal imaging of PC12 cells. (A) PC12 cells were pretreated with 10 mM glutamate for different times, and then cells were incubated with 100 μM MI-H$_2$O$_2$ and 100 μM LY-H$_2$O$_2$ for 40 min. (B) The fluorescence intensity output of MI-H$_2$O$_2$ in panel A. (C) The fluorescence intensity output of LY-H$_2$O$_2$ in panel A. (D) The Gcase activity in cell extract. (E) The Gcase activity in mouse brain tissue. MI-H$_2$O$_2$ (100 μM, λ_{ex} = 633 nm, λ_{em} = 650 nm-750 nm), LY-H$_2$O$_2$ (100 μM, λ_{ex} = 405 nm, λ_{em} = 410 nm-500 nm). Scale bar = 50 μm.
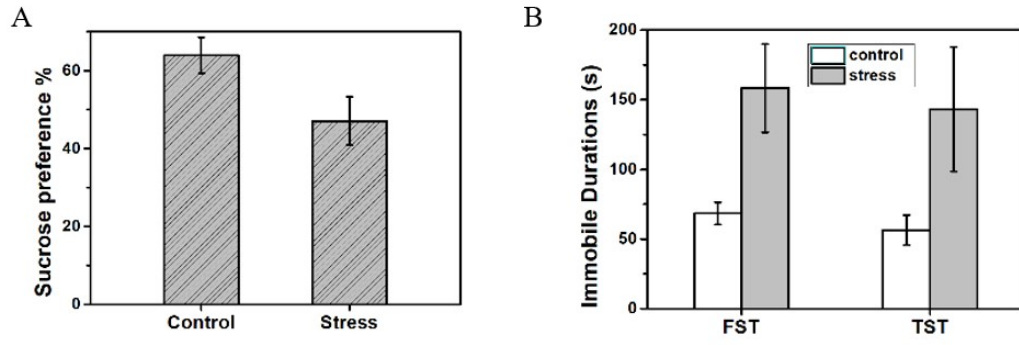
Figure S14 Depression-like behaviors tests of mice. (A) Sucrose preference test of mice with and without CORT. (B) Immobile time of forced swimming test and tail suspension test in behaviors tests. The data are expressed as the mean ± S.D. 10 mice in each group.
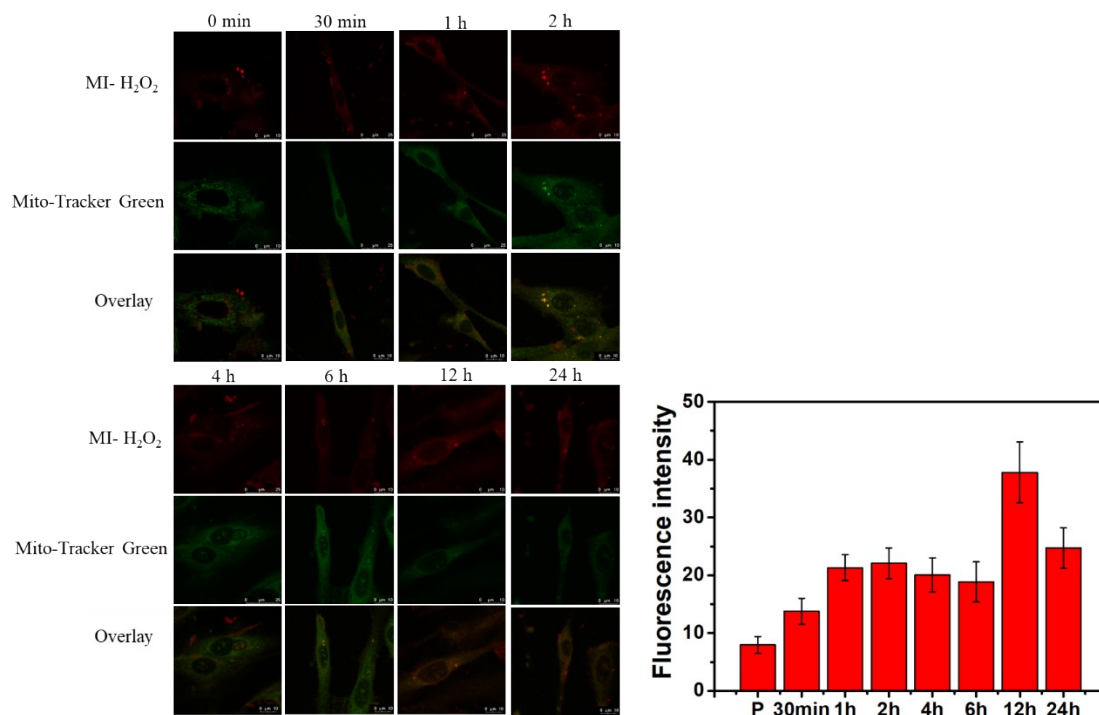
Figure S15 Co-localization fluorescence images of PC12 cells stained with MI-H_2O_2 and Mito-Tracker Green after being induced with Glu. First, PC12 cells were stained with Glu (10 mM, 0 min, 30 min, 1 h, 2 h, 4 h, 6 h, 12 h, 24 h), then treated with MI-H_2O_2 (100 μM) and Mito-Tracker Green (100 nM) for 40 min. MI-H_2O_2 (100 μM, λ_{ex} = 633 nm, λ_{em} = 650–750 nm), Mito-Tracker Green (100 nM, λ_{ex} = 488 nm, λ_{em} = 495–550 nm), Scale bar = 10 μm.
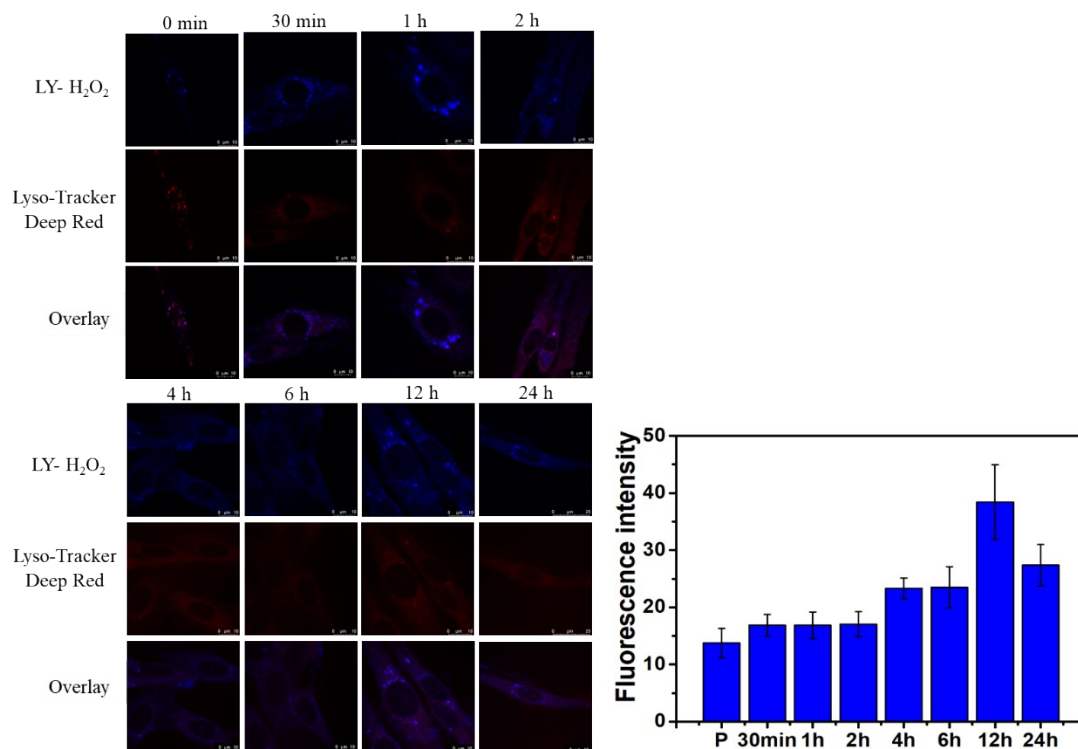
Figure S16 Co-localization fluorescence images of PC12 cells stained with LY-H$_2$O$_2$ and Lyso-Tracker Deep Red after being induced with Glu. First, PC12 cells were stained with Glu (10 mM, 0 min, 30 min, 1 h, 2 h, 4 h, 6 h, 12 h, 24 h), then treated with LY-H$_2$O$_2$ (100 μM) and Lyso-Tracker Deep Red (100 nM) for 40 min. LY-H$_2$O$_2$ (100 μM, λ_{ex} = 405 nm, λ_{em} = 410–500 nm), Lyso-Tracker Deep Red (100 nM, λ_{ex} = 633 nm, λ_{em} = 650–750 nm), Scale bar = 10 μm.
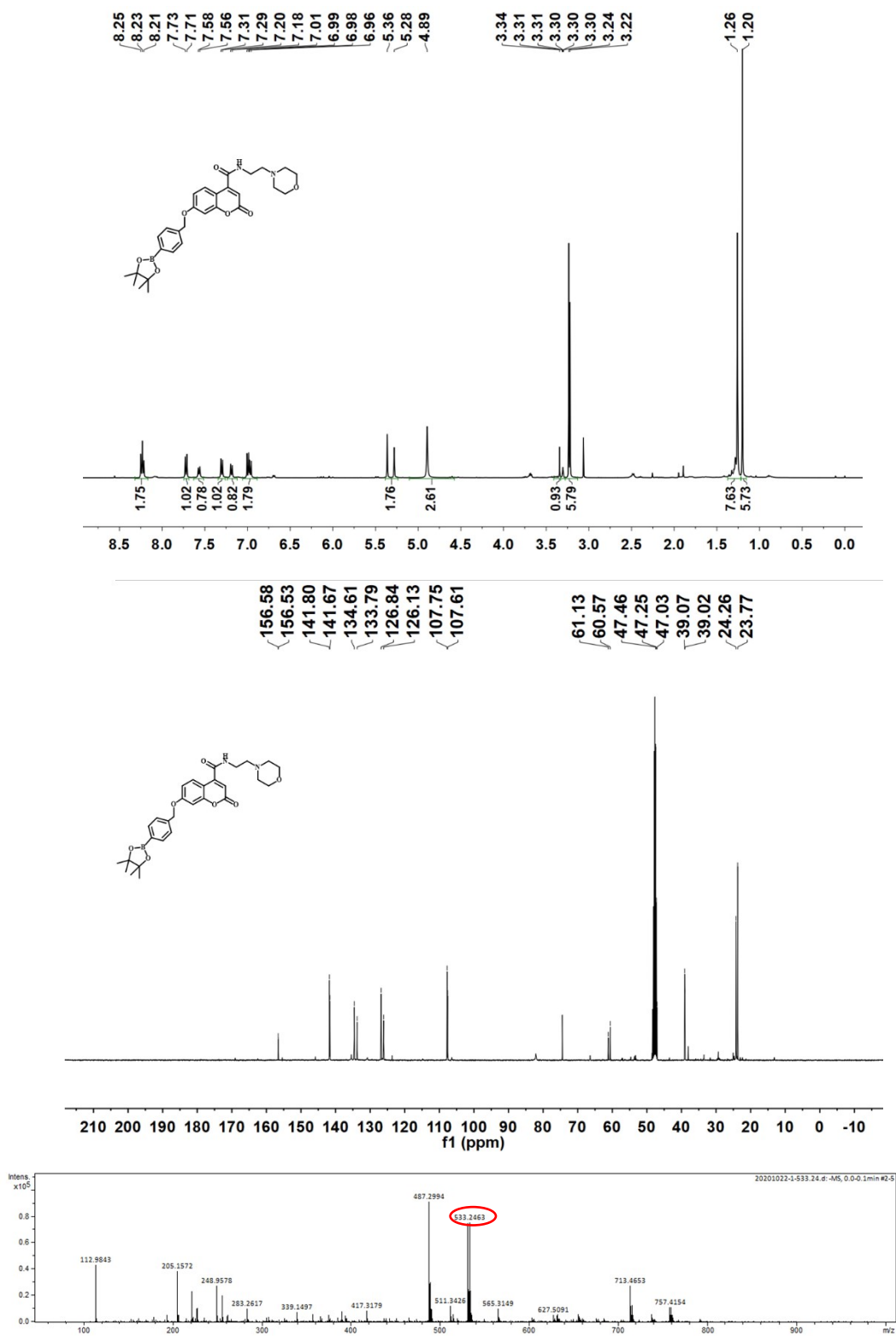
Figure S17 ^{1}HNMR, ^{13}CNMR, and HRMS of LY-H$_2$O$_2$
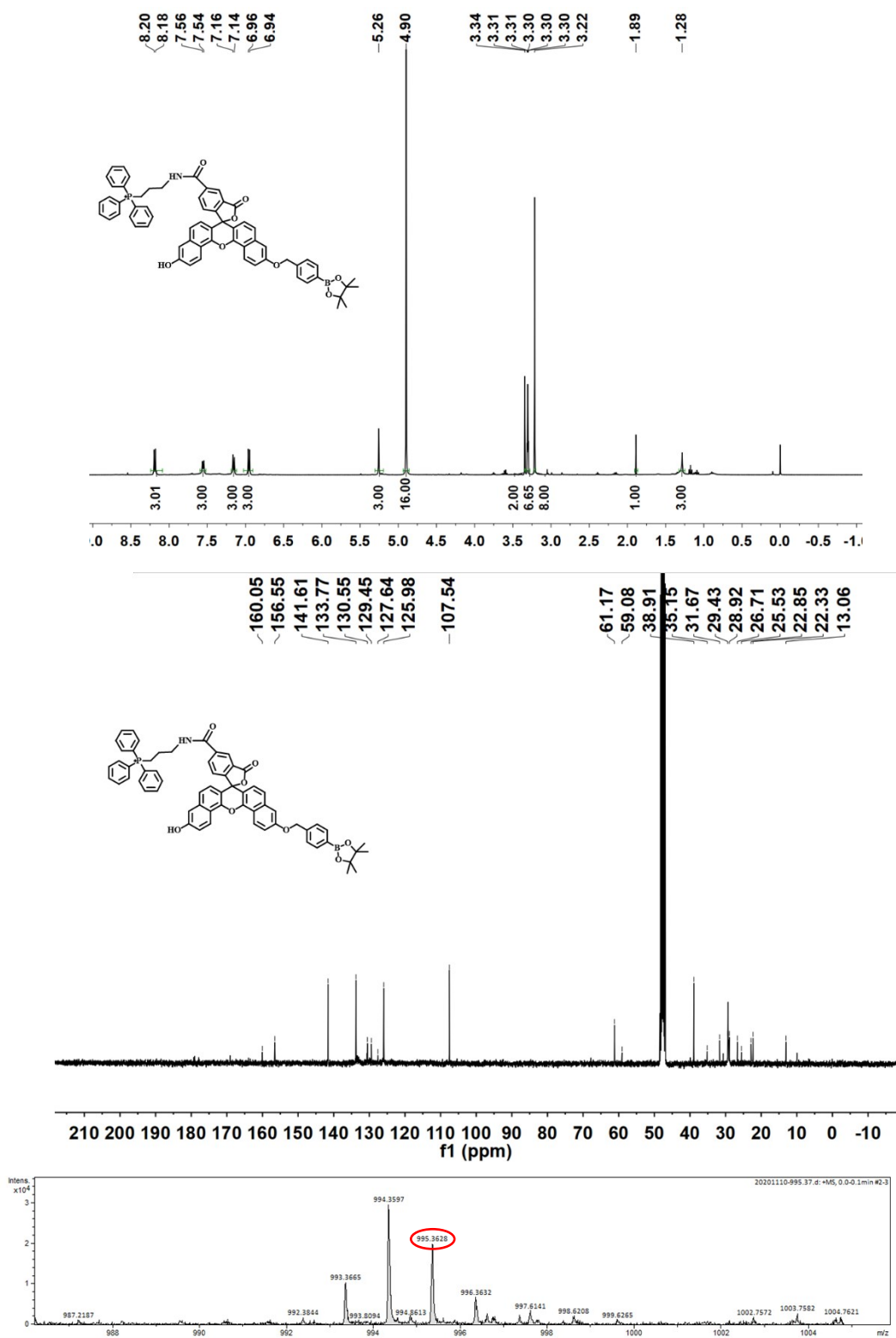
Figure S18 ^{1}HNMR, ^{13}CNMR, and HRMS of MI-H$_2$O$_2$

Reference

[1] H. Maeda, K. Yamamoto, Y. Nomura, I. Kohno, L. Hafsi, N. Ueda, S. Yoshida, M. Fukuda, Y. Fukuyasu, Y. Yamauchi. A design of fluorescent probes for superoxide based on a nonredox mechanism. *J. Am. Chem. Soc.*, **2005**, 127: 68-69.

[2] D. Oushiki, H. Kojima, T. Terai, M. Arita, K. Hanaoka, Y. Urano, T. Nagano. Development and application of a nearinfrared fluorescence probe for oxidative stress based on1 differential reactivity of linked cyanine dyes. *J. Am. Chem. Soc.*, **2010**, 132: 2795-2801.

[3] S. Kim, R. Dicosimo, J.S. Filippo. Spectrometric and chemical characterization of superoxide. *Anal. Chem.*, **1979**, 51: 679-681.

[4] M. N. Hughes, H.G. Nicklin. The chemistry of pernitrites. Part I. Kinetics of decomposition of pernitrous acid. *J. Chem. Soc. (A)*, **1968**: 450-452.

[5] P. S. Dixit, K. Srinivasan. The effect of clay-support on the catalytic epoxidation activity of a manganese(III)-Schiff base complex. *Inorg. Chem.*, **1988**, 27: 4507-4509.

[6] M. G. Steiner, C. F. Babbs. Quantitation of the hydroxyl radical by reaction with dimethyl sulfoxide. *Arch. Biochem. Biophys.*, **1990**, 278: 478-481.

[7] N. Adarsh, M. Shanmugasundaram, R. R. Avirah, D. Ramaiah. Aza-BODIPY derivatives: enhanced quantum yields of triplet excited states and the generation of singlet oxygen and their role as facile sustainable photooxygenation catalysts. *Chem.-Eur. J.*, **2012**, 18: 12655-12662.

[8] X. Y. Lu, C. S. Kim, A. Frazer, W. Zhang. Leptin: a potential novel antidepressant. *Proc. Natl. Acad. Sci. U. S. A.*, **2006**, 103: 1593-1598.

[9] B. Petit-Demouliere, F. Chenu, M. Bourin. Forced swimming test in mice: a review of antidepressant activity. *Psychopharmacology*, **2005**, 177: 245-255.

[10] T. Chen, X. Pei, Y. Yue, F. Huo, C. Yin. An enhanced fluorescence sensor for specific detection Cys over Hcy/GSH and its bioimaging in living cells. *Spectrochimica Acta Part a-Molecular and Biomolecular Spectroscopy*, **2019**, 209: 223-227.

[11] T. Yamada, S. Fujiwara, K. Fujita, Y. Tsuchido, T. Hashimoto, T. Hayashita. Development of Dipicolylamine-Modified Cyclodextrins for the Design of Selective Guest-Responsive Receptors for ATP. *Molecules*, **2018**, 23: 635.